SANS Investigations of Topological Constraints in Networks Made from Triblock Copolymers

S. Westermann, V. Urban, W. Pyckhout-Hintzen,* and D. Richter

Forschungszentrum Jülich, Institut für Festkörperforschung, Postfach 1913, D-52425 Jülich, Germany

E. Straube

Martin-Luther-Universität Halle-Wittenberg, Fachbereich Physik, D-06099 Halle, Germany

Received February 14, 1996; Revised Manuscript Received June 17, 1996[⊗]

ABSTRACT: A theoretical and experimental investigation of the SANS structure factor of labeled triblock HDH copolymer chains, randomly cross-linked into a network, is presented. We combine the RPA method for the consideration of the strong interchain correlations and the tube model with a harmonic deformation dependent constraining potential, modeling the action of cross-links and entanglements. With this approach a successful description of the scattering behavior under strain is achieved. The sensitivity of the method allows the detection of chain splittings during cross-linking with peroxides.

Introduction

Recent work showed that a detailed understanding of rubber elasticity can be achieved by the analysis of the form factor $S(\vec{q})$ of a single chain under strain inside the polymer network.[1−4] Especially the wave vector range of the small-angle neutron scattering (SANS) allows the investigation of both the chain deformation and the chain fluctuations on a length scale which is suitable for a test of crucial assumptions of current theories of rubber elasticity. The analysis of two-dimensional neutron-scattering patterns from networks made by random cross-linking permitted the determination of the dimensions of a confinement tube[5] and its deformation dependence under strain.[6] While the chain dimensions deform affinely, the tube constraints undergo subaffine deformations and follow a square-root dependence in the strain.[6]

The investigation of networks made up from triblock copolymers of alternating blocks of protonated and deuterated monomers opens the interesting possibility of changing the length of the labeled path without affecting network properties. The use of triblock copolymers with a labeled middle block excludes any effect of dangling ends on the scattering properties. Additionally the length of the labeled path can be chosen to comply with the accessible q range. Especially, also for long primary chains which are necessary for good network properties the scattering in extension direction remains in the observable range.

To counteract low scattering intensities as N, the number of labeled monomers, decreases, measurements on pure triblock systems are preferable. These systems show the well-known correlation hole,[7] which can be described for undeformed melts or networks perfectly by the de Gennes RPA method.[8,9] Due to the pronounced peak structure the scattering properties are also highly sensitive to strain as already shown in a first experimental investigation of a similar un-cross-linked PS system several years ago by Boue,[10] who observed shifts and deformations of the peaks whereas a quantitative interpretation of the phenomena was lacking. This peak structure offers an additional advantage, because it can be expected that the deformation dependence of the tubes will be reflected particularly in the peak region.

The reported work concerns (i) SANS investigations on networks made by randomly cross-linking of long monodisperse primary chains with labeled middle blocks which are long in comparison to the tube dimensions and (ii) results of a combination of an RPA description of the interchain correlations with the tube model[6] and its treatment within the Warner−Edwards approach.[11]

The paper is organized in the following manner: First, the application of the tube model to the SANS measurements on a network made from a diluted blend of labeled homopolymers will be referred to. Second, the combination of the RPA correction[8,12,13] and the Warner−Edwards approach[11] will be discussed and an expression for the structure factor of a network from triblock chains under strain will be derived. Finally the experimental results on HDH polyisoprene (PI) and a comparison with the developed theory will be given. The results show that the proposed copolymer systems are very valuable tools for a profound investigation of confinement effects in bulk polymers.

Tube Model for Networks

Combining the Warner−Edwards approach[11] for the calculation of the form factor of a single labeled path in a network and the tube picture for the description of the lateral confinement of the network chains,[6,14,15] the following characteristics of the tubes and especially the deformation dependence were found:

(i) The tube diameters in the network are somewhat smaller than the tubes in melts as deduced from viscoelastic data[5] and neutron spin−echo measurements.[16,17]

(ii) The tubes are deformed nonaffinely in relation to the macroscopic network deformation and a typical lozengic shape of two-dimensional scattering patterns at large deformations in the intermediate small-angle regime is observed.[18]

(iii) In scattering experiments the tube confinement can be observed as mean-square displacements along the scattering direction $\vec{q}$:

$$d_\phi^2 = \langle (R_\phi(s) - \lambda_\phi \hat{R}_\phi(s))^2 \rangle \qquad (1)$$

relatively to a displaced mean configuration $\lambda_\phi \hat{R}(s)$,

[⊗] Abstract published in *Advance ACS Abstracts,* August 15, 1996.

S0024-9297(96)00238-0 CCC: $12.00

where $\vec{q}$ is the scattering vector, ϕ is the angle between $\vec{q}$ and the direction of the uniaxial extension λ of the sample. The experimental results show a very good agreement with the prediction of a mean-field approach:

$$d_\phi = d_0 \lambda_\phi^{\nu} \tag{2}$$

with the exponent $\nu = {}^1/_2$ expressing the nonaffinity of the tube deformations and

$$\lambda_\phi{}^2 = \lambda^2 \cos^2(\phi) + (1/\lambda)\sin^2(\phi) \tag{3}$$

as effective extension ratio[19] into the observed direction.

Structure Factor

We will use the Warner−Edwards approach[11] as the theoretical basis for the calculation of the structure factor of a labeled path in a network. The approach allows the introduction of the RPA corrections to the structure factor of the network in a very convenient way. For a single labeled path in a network the form factor $S(\vec{q},\lambda)$ can be written

$$S(\vec{q},\lambda) = 2\int_0^1 \mathrm{d}x \int_0^x \mathrm{d}x' \prod_\mu \exp\left[-(Q_\mu\lambda_\mu)^2(x-x') - Q_\mu{}^2(1-\lambda_\mu{}^2)\left\{\frac{d_\phi{}^2}{2\sqrt{6}R_g{}^2}\left(1-\exp-\frac{(x-x')}{d_\phi{}^2/2\sqrt{6}R_g{}^2}\right)\right\}\right] \tag{4}$$

where R_g is the radius of gyration of the labeled path and $Q_\mu = q_\mu R_g$ is a component of the reduced scattering wave vector in the main axis system of the deformation tensor. x and x' are dimensionless contour length coordinates extending over the labeled paths of the chains.

Equation 4 was previously obtained by averaging the contributions of chains with different mean configurations over the random-flight distribution of these configurations using the replica method. Equation 4 reflects this approach and can be interpreted as the product of the form factor of a deformed random path $\exp[-(Q_\mu\lambda_\mu)^2(x-x')]$ and the contributions from the restricted fluctuations around this path.

A single-component system consisting of pure triblock copolymer chains with a labeled middle block but with chemically identical segments shows zero scattering intensity at zero scattering angle. Fluctuations at large length scales are suppressed due to the incompressibility of the system.[7,8] Correlations of this kind are not considered within the Warner−Edwards approach where the average configurations of the labeled chains are assumed to be random as is well proven in diluted systems. However, these correlations (the correlation hole) can be treated perfectly by the de Gennes RPA method. The success of this approach is founded on the fact that the intrachain correlations in such a block copolymer system remain unchanged. From this follows that the self-consistent potential describing the interchain correlations is the same for all segments of the chains. As a consequence the fluctuations on the length scale of the chain and especially on the length scale of the tube dimensions are statistically independent of the long-range correlations between the chains.

On the basis of these considerations, the following modifications are introduced into the Warner−Edwards approach[11] for the calculation of the structure factor of a network made of statistically cross-linked monodisperse HDH PI triblock copolymers:

(i) By application of the concept of the RPA approach,[7,12] dealing with the correlation hole effect, to our problem, the form factor of a single deformed path in a network according to eq 4 may be modified by the corresponding RPA structure factor. The form factor $S(\vec{q},\lambda)$ of the labeled path (eq 4) has to be multiplied by the RPA corrected structure factor of the deformed copolymer system with the labeled middle block and divided by the form factor of the isolated middle block.

$$S(\vec{q},\lambda) \rightarrow S_{22,\mathrm{RPA}}(\vec{q},\lambda)/S_{22}(\vec{q}\lambda) \times S(\vec{q},\lambda) \tag{5}$$

By this modification $S(\vec{q},\lambda)$ represents the structure factor of the triblock system obtained under the assumption that the restricted chain fluctuations due to tube effects and the long-range correlations caused by the incompressibility of the system are statistically independent.

(ii) $S_{22,\mathrm{RPA}}(\vec{q},\lambda)$ is calculated without interaction corrections according to

$$S_{22,\mathrm{RPA}} = S_{22} - \frac{\sum_{i=1}^{3} S_{i2} \times \sum_{j=1}^{3} S_{2j}}{\sum_{i,j=1}^{3} S_{ij}} \tag{6}$$

where the S_{ij} are the contributions from blocks i and j to the form factor of a triblock random chain.[12]

(iii) For symmetrical triblocks, these contributions read

$$S_{11} = S_{33} = (2N_w{}^2/Q_w{}^2)[1 - (1 - \exp(-Q_w{}^2))/Q_w{}^2] \tag{7}$$

$$S_{12} = S_{23} = (N_w N_m/Q_w{}^2 Q_m{}^2)[1 - \exp(-Q_w{}^2)][1 - \exp(-Q_m{}^2)] \tag{8}$$

$$S_{13} = (N_w{}^2/Q_w{}^4)[1 - \exp(-Q_w{}^2)]^2 \exp(-Q_m{}^2) \tag{9}$$

$$S_{22} = (2N_m{}^2/Q_m{}^2)[1 - (1 - \exp(-Q_m{}^2))/Q_m{}^2] \tag{10}$$

were N_w and N_m denote the numbers of statistical segments in a wing and in the middle part of the block copolymer (with $f = N_m/(2N_w + N_m)$) and $Q_{w/m} = |\vec{q}\lambda|R_{g,w/m}$, the corresponding dimensionless scattering vectors.

The general assumptions of the presented approach will be tested with the investigated triblock system. These are the separability of (i) interchain contributions to the distribution function of the mean configurations and (ii) contributions from the restricted fluctuations about these mean configurations, only.

Experiments

Sample Preparation. Monodisperse polyisoprene (PI) was prepared by standard anionic polymerization in apolar solvent under high-vacuum conditions. The initiator was monofunctional *sec*-BuLi, and a triblock structure was achieved by subsequent addition of carefully weighted amounts of protonated monomers for the wing part and deuterated monomer forming the center block. The living anion after addition of the third block was deactivated with degassed methanol. SEC measurements (Waters-Millipore, 150 C) were performed in THF and the molecular weight M_w was determined to be 136 000 ± 4500 g/mol from a narrow PI standards calibration.

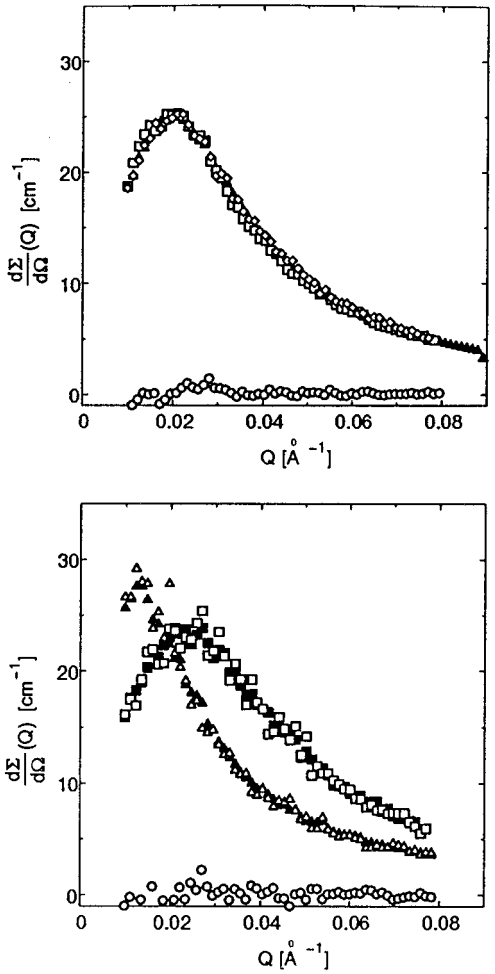

Figure 1. Check of the validity of the transversal Zimm-type extrapolation: (a, top) Comparison of the radial averaged sample (closed triangles) and the extrapolated data for the x (□) and y (◇) axis. The open circles represent the difference between x axis data and original data. (b, bottom) Comparison of the original axis data of a deformed sample with $\lambda = 1.75$ (open symbols) and the extrapolated data (closed symbols) in parallel (triangles) and perpendicular (squares) direction. The open circles represent the difference for the perpendicular direction.

The total polydispersity was $u = 1.012$ and a stoichiometric conversion of the added monomer confirmed. From this observation, asymmetry in the length of the wings will be negligible. The molecular weight M_w was determined by low-angle laser light scattering (Chromatix KMX-6) to be 134 600 ± 1700 g/mol with dn/dc = 0.099 ± 0.001 as measured from dilute solutions in cyclohexane and extrapolation to $c = 0$ (Chromatix KMX-16). The average deuterium fraction from SEC, chemistry, and light scattering, corrected for the density, is $f = 0.37 \pm 0.02$, whereas from the differential refraction index using a weighting of pure H- and D-PI, $f = 0.38 \pm 0.02$.

Statistical networks were prepared from the pure triblock copolymer assuming the formation of one cross-link per molecule of cross-linker dicumyl peroxide (DCP).[20,21] Polymer and cross-linker were dissolved in THF (20%) and transferred to a Teflon mould. The solvent was taken off in vacuum for several days, and finally the system was cured in Ar atmosphere at 163 °C for 2 h to ensure complete decomposition of the peroxide. The cross-link density was estimated from swelling in cyclohexane and yields 6450 ± 250 g/mol with a gel fraction $w_{gel} = 0.972 \pm 0.005$. The ratio of cross-link/DCP molecule was 1.08 ± 0.03.

SANS. The small-angle neutron-scattering experiment on the un-cross-linked melt was performed using the NG7 instrument at the National Institute of Standards and Technology in Gaithersburg, MD, with a neutron wavelength of $\lambda_N = 6.0$ Å, with a wavelength spread of about 9%. The data were converted to absolute intensities by means of a calibrated silica standard. The detector distances were 3.6 and 15.3 m providing an experimental range of 0.003 Å$^{-1} \le q \le$ 0.09 Å^{-1} in terms of the scattering vector $q = (4\pi/\lambda_N)\sin\theta/2$, θ being the scattering angle.

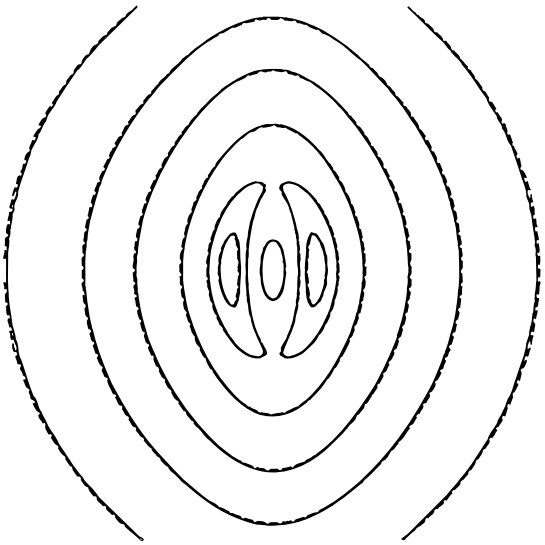

Figure 2. Comparison between the spline-interpolated data (- - -) and the theoretical curve (—). Even in the peak region, the agreement is excellent.

The cross-linked polyisoprene networks were studied at the PAXY instrument at LLB, Saclay, France, using a neutron wavelength of 8.0 Å with a wavelength spread of 10%. The detector distance was 3.2 m covering a q range of 0.007 Å$^{-1} \le q \le$ 0.09 Å^{-1}. The absolute calibration was performed against a separately measured water sample of 1 mm thickness.

The isotropic cross-linked sample was remeasured at the KWS1 instrument at the FRJ-2 reactor in KFA, Jülich, at a wavelength of 7.0 Å with a wavelength spread of $\Delta\lambda_N/\lambda_N = 22\%$. The detector distances were 8 and 20 m giving an experiment range of 0.003 Å$^{-1} \le q \le$ 0.04 Å^{-1}. The data were absolutely calibrated by means of a secondary polyethylene standard.

Macroscopic strains were determined within 5% accuracy from a grid of marks on the sample. The experimental lengths-to-widths ratios upon straining were in absolute agreement with an affine sample deformation. The macroscopic sample deformation was checked by means of the measured sample transmission as the thickness changes with $1/\sqrt{\lambda}$, assuming incompressibility.

Data Treatment. The raw data were normalized for monitor counts and corrected for background, empty beam, empty cell (in case of the melt), and detector sensitivity. The incoherent scattering was determined separately from a 100% protonated PI network sample of comparable cross-link density and subtracted weighted with its volume fraction.

The observed differential cross section dΣ/d$\Omega(\vec{q},\lambda)$ is related to the structure factor $S(\vec{q},\lambda)$ by

$$\frac{d\Sigma}{d\Omega}(\vec{q},\lambda) = \frac{\Delta\rho^2 V_w f}{N_A} S(\vec{q},\lambda) \qquad (11)$$

$\Delta\rho^2$ being the contrast factor, given by $N_A[n(b_D - b_H)/\Omega_0]^2$. b_H and b_D are the nuclear coherent scattering lengths for hydrogen and deuterium, n is the number of exchanged hydrogens per monomer of molar volume Ω_0, and V_w is the weight-average molar volume of the labeled middle block of the polymer.

The values of the double integral of eq 4 were calculated by application of the subroutine RAKU from the Zentralabteilung für Angewandte Mathematik (ZAM) of the Forschungszentrum Jülich.

In the case of isotropic samples, the data were radially averaged and fitted by eq 4 with $\lambda = 1$, converting the

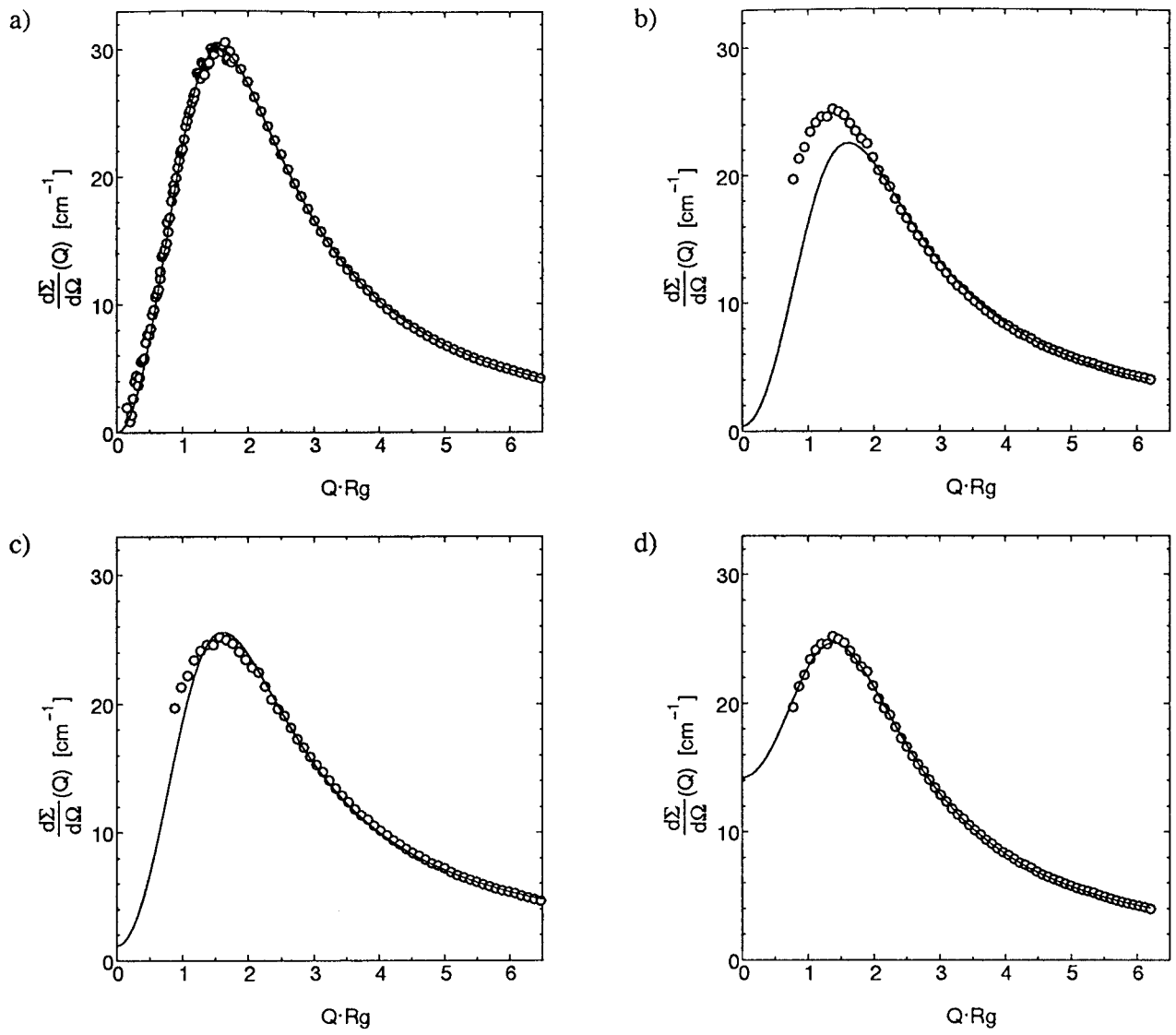

Figure 3. (a) Radial averaged neutron scattering data from the HDH copolymer melt. The fit is calculated by the RPA approach, giving $R_G = 70.5$ Å. (b) Radial averaged neutron-scattering data from the isotropic network sample. The fit following the RPA approach with $R_G = 70.5$ Å is no longer able to describe the data. (c) Fit following the RPA approach with a fitted value for the radius of gyration of $R_G = 80 \pm 1$ Å. The peak structure is still not represented quite well. (d) The introduction of a possible chain splitting process during cross-linking to the RPA equation now gives a good fit with reasonable parameters (see Table 1). The fitted amount of scission is $w_s = 0.08$.

scattering behavior to an RPA-corrected Debye curve. The determined radius of gyration was used for fitting the anisotropic data. The fitted prefactor was compared with its expected value. An additional background constant was allowed to fit, to correct, e.g., for incoherent scattering of the deuterium and experimental uncertainties in the labeled fraction.

To evaluate the experimental results of the deformed samples two methods of data treatment were undertaken:

(i) For fits along the principal deformation axes, in contrast to conventional sector averaging with opening angles of about 10−20°,[22] we performed a transversal Zimm-type extrapolation of the experimental data using the q^2 dependence around the axis according to

$$S^{-1}(q_1,q_2) = S^{-1}(q_1,0)\left(1 + \frac{R_{G,\mathrm{app}}{}^2(q_1)}{3} q_2{}^2\right) \qquad (12)$$

where q_1 and q_2 stand for $q_{\parallel}$ and $q_{\perp}$, respectively, and $S(q_1,0)$ is the axis value of interest. This is valid in the range of $q_{\parallel,\perp} \cdot R_{G\parallel,\perp} \approx 1$ perpendicular to the axis under consideration. The stability of this procedure was tested by comparison of the extrapolated data with a radially averaged sample as well as with the original axis values of the scattering intensities of a deformed sample as demonstrated in Figure 1. The extrapolated data were simultaneously fitted in both directions using eq 4 and assuming incompressibility for the determination of the corresponding extension ratios.

(ii) Further, we performed two-dimensional fits in the q_x, q_y plane by eq 4. Applying the IMSL routine BS2IN, the theoretical data were splined on a grid of 26 × 26 points in one quadrant of the q plane with narrower meshes in the neighborhood of the correlation peak position. The obtained spline coefficients were used to interpolate the data at the original experimental points by means of the procedure BS2VL of the IMSL library. The accuracy of this procedure is demonstrated in Figure 2.

By use of the routine UMPOL (IMSL), the absolute difference between the fit curve and the experimental points was minimized.

In all cases, d_0 was the only relevant fit parameter, as R_G, the prefactor, and the background were fixed to their values determined in the isotropic case. No Flory−Huggins parameters were necessary for the PI system.[3]

Results and Discussion

Scattering on Melts and Undeformed Networks. Figure 3a−d shows the radial averaged scattering from

Table 1

sample	w_s	R_G [Å]
melt, un-cross-linked	0	71.0 ± 0.5
network, $\lambda = 1$	0	80.0 ± 0.5
network, $\lambda = 1$	0.09	70.5 ± 0.5
network, $\lambda = 1$, KWS1	0.075	70.5 ± 0.5

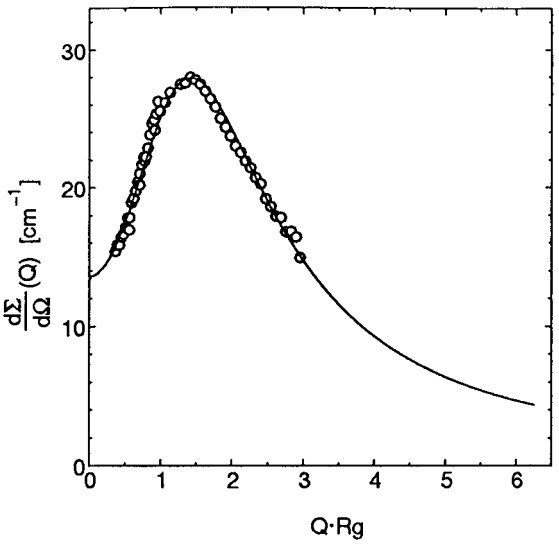

Figure 4. Radial averaged neutron-scattering data from the isotropic network sample measured at the KWS1 machine at the FRJ-2 reactor in KFA, Jülich. As smaller q values were obtained, the effect of chain splitting is confirmed. The fit results are given in Table 1.

the copolymer melt and the corresponding undeformed network. In Figure 3a the scattering data from the uncross-linked melt are shown together with the best fit with the RPA structure factor according to eq 6. The radius of gyration of the labeled middle block is fitted to be 71.0 ± 0.5 Å. This result is in very good correspondence with the expected value, $R_G = 72 \pm 2$ Å, calculated from the molecular weight, assuming a characteristic ratio of $C_\infty = 5.1$.[23] Keeping this value fixed, we tried to fit the scattering data of the isotropic network sample. It can clearly be seen from Figure 3b that the theory is not able to represent the data. Fitting R_G, a best-fit value of $R_G = 80 \pm 1$ Å is obtained, which is much larger than the predicted value and therefore can be rejected. The comparison between theory and experiment is demonstrated in Figure 3c, which shows clear discrepancies in the peak region and a clear tendency to nonzero intensity at $\vec{q} \to 0$. These deviations are larger than all possible experimental uncertainties. Resolution effects[24] were considered but were not able to reproduce the observed discrepancy. Polydispersity[9] could be discarded due to the absence of any sign of polydispersity in the melt. Consequently, the different behavior must be caused by changes of the system during cross-linking. The buildup of concentration fluctuations of clusters of labeled parts of the triblock chains can be discarded due to the incompressibility of the system. Indeed, the success of the RPA method proves that thermal concentration fluctuations are negligibly small in undiluted triblock systems. Therefore, in a system with unchanged chains, concentration fluctuations can also not be frozen in during the cross-linking process. One possible reason for changes of the system and a likely explanation for the experimental results is random chain splitting caused by the used peroxide cross-linker because already a small amount of different chains in the system will cause long-range concentration fluctuations and nonzero intensity at $\vec{q} \to 0$ to show up. Chain splitting during cross-linking with DCP is well-known for polyolefins but still discussed for polydienes, for which it rather behaves as a model cross-linker.[25,26]

The RPA structure factor of a system consisting of a fraction w_s of chains splitted with equal probability at any monomer reads

$$\bar{S}_{22,\mathrm{RPA}} = (1 - w_s)\bar{S}_{\mathrm{RPA,to}} + w_{sw}\bar{S}_{\mathrm{RPA,ts}} + 2w_{sm}\bar{S}_{\mathrm{RPA,d}} \tag{13}$$

where $w_{sw} = (1 - f)w_s$ is the probability for a scission reaction in the hydrogenous part of the chain (the wings) and $w_{sm} = fw_s$ the corresponding probability of splitting of the labeled middle part, f being the fraction of deuterated monomers per chain. $\bar{S}_{\mathrm{RPA,to}}$ is the structure factor of the remaining unsplitted triblock chains. Changes in comparison to eq 6 must be made in the nominator only by replacing

$$\sum_{i,j=1}^{3} S_{ij} \to (1 - w_s)\sum_{i,j=1}^{3} S_{ij} + w_{sw}(\bar{S}_h + \sum_{i,j=1}^{3} \bar{S}_{ij,\mathrm{ts}}) + 2w_{sm}\sum_{i,j=1}^{2} \bar{S}_{ij,\mathrm{d}} \tag{14}$$

This modified nominator with weighted extra contributions is the same for all terms on the right-hand side of eq 13. In eq 14, $\bar{S}_h$ is the averaged form factor of an ensemble of homopolymer chains produced by random splitting of the triblock copolymer in the wing parts. $\sum_{i,j=1}^{3}\bar{S}_{ij,\mathrm{ts}}$ denotes the contributions of the remaining part of a triblock chain with one wing of variable length. It has the same structure as the corresponding contributions in eq 6 with the replacements

$$S_{11} \to \bar{S}_{11} \neq S_{33} \tag{15}$$

$$S_{12} \to \bar{S}_{12} \neq S_{23} \tag{16}$$

$$S_{13} \to \bar{S}_{13} \tag{17}$$

The expressions for the averaged form factors $\bar{S}_{ij}$ are given below. Analogously $\sum_{i,j=1}^{2}\bar{S}_{ij,\mathrm{d}}$ denotes the contributions of a diblock chain produced by splitting within the middle part. It has again the same structure as the corresponding contributions in eq 6 with the replacements

$$S_{11} \to 0 \tag{18}$$

$$S_{12} \to 0 \tag{19}$$

$$S_{13} \to 0 \tag{20}$$

$$S_{22} \to \bar{S}_{22} \tag{21}$$

$$S_{23} \to \bar{S}_{23} \tag{22}$$

also given below.

The contribution of the modified triblock chains to the structure factor $\bar{S}_{\mathrm{RPA,ts}}$ in eq 13 is again given by an expression analogous to eq 6 with the replacements according to eqs 15−17 but now also in the denominator. Splitting in the middle block produces diblock copolymers with the contribution $\bar{S}_{\mathrm{RPA,d}}$ in eq 13. It is obtained

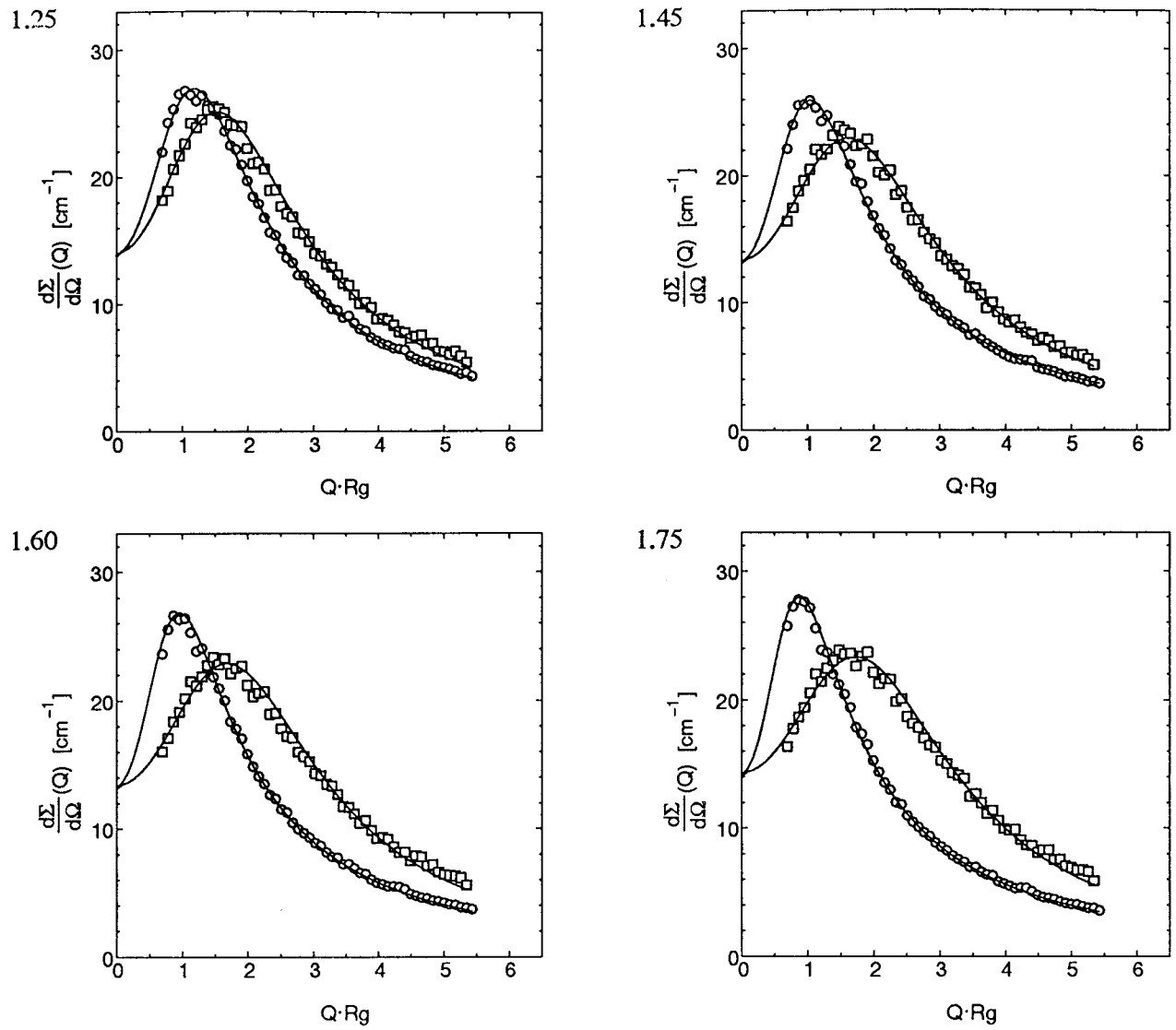

Figure 5. Experimental results in parallel (circles) and perpendicular (squares) direction to the strain for the four strains applied. The experimental data were obtained by use of the transversal Zimm-type extrapolation. The fitted tube diameter is 42 ± 1 Å (see Table 2).

analogously to $\bar{S}_{RPA,ts}$ with the replacements according to eqs 18−22.

The averaged form factors $\bar{S}_{ij}$ are obtained by integration over the segment numbers of the chains and normalization. We obtained

$$\bar{S}_{11} = \bar{S}_h = (N_w^2/Q_w^2)[1 - 2(1 - (1 - \exp(-Q_w^2))/Q_w^2)/Q_w^2] \quad (23)$$

$$\bar{S}_{12} = (N_w N_m/Q_w^2 Q_m^2)[1 - (1 - \exp(-Q_w^2))/Q_w^2][1 - \exp(-Q_m^2)] \quad (24)$$

$$\bar{S}_{13} = (N_w^2/Q_w^4)[1 - \exp(-Q_w^2)][1 - (1 - \exp(-Q_w^2)/Q_w^2]\exp(-Q_m^2) \quad (25)$$

$$\bar{S}_{22} = (N_m^2/Q_m^2)[1 - 2(1 - (1 - \exp(-Q_m^2))/Q_m^2)/Q_m^2] \quad (26)$$

$$\bar{S}_{23} = (N_m N_w/Q_m^2 Q_w^2)[1 - (1 - \exp(-Q_m^2))/Q_m^2][1 - \exp(-Q_{w2})] \quad (27)$$

Table 2

	w_s		d_0 [Å]	
λ	2d	axes	2d	axes
1.25 ± 0.05	0.072	0.070	41.5	42.2
1.45 ± 0.05	0.072	0.072	41.6	42.4
1.60 ± 0.05	0.072	0.072	41.6	42.4
1.75 ± 0.05	0.072	0.075	41.5	41.5

The best fit of the experimental data considering this correction to the RPA structure factor is shown in Figure 3d. The resulting value for the radius of gyration of R_G = 70.5 ± 0.5 Å is in good correspondence with the expected value, R_G = 72 ± 2 Å. With an optimized content of scissioned chains of w_s = 0.09, the agreement is good and the fit results correspond well to those obtained from the un-cross-linked melt (see Table 1). The chain scissioning is considerably less than 0.21 as was estimated indirectly from a consideration of the influence of scissioned chains on the entanglement contributions on stress−strain data[27] which is based on a number of assumptions especially on the entanglement contributions in defect-containing networks.

This small amount of chain splitting justifies the assumption of only one single random scission per primary chain and explains why this effect cannot be

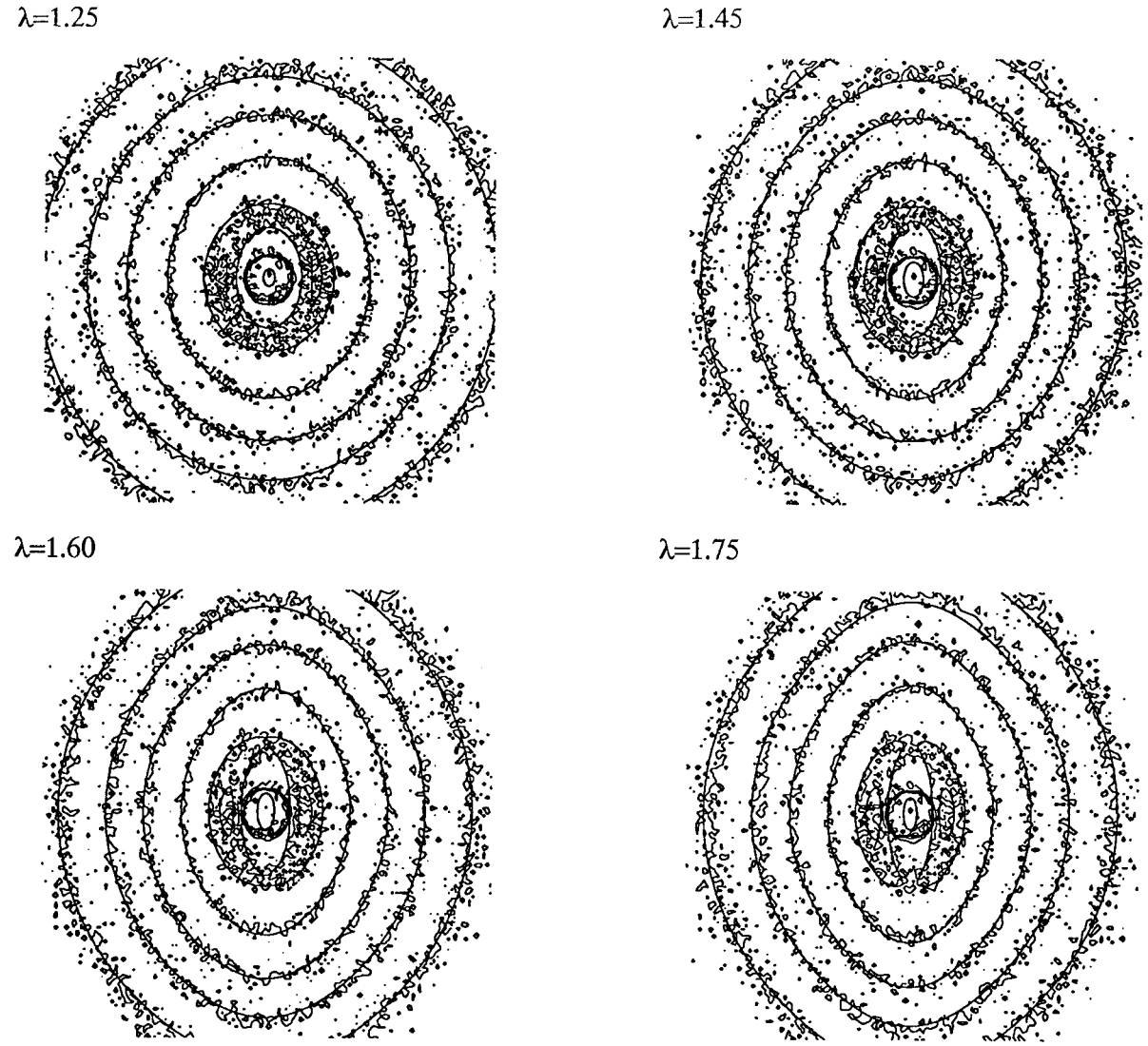

Figure 6. Contour plots of the two-dimensional data fits. The agreement is excellent and the results compare well with those obtained from the axes fits (see Table 2).

observed by other methods. E.g, only small changes of the sol fraction and a somewhat higher content of short chains in the sol fraction can be expected. A systematic study of the thermal degradation in polyisoprene networks and melts, whether or not inhibited with the appropriate antioxidant, is under preparation.[28] First results clearly show the increase of intensity at low q at decreasing peak intensity as a function of annealing time.

Figure 4 shows a fit on scattering data at the KWS1 instrument at the FRJ-2 reactor in KFA, Jülich. Compared to the Saclay measurements, smaller q values were achieved, which confirm the effect of chain splitting unambiguously and a chain splitting of 0.075 (see Table 1) was found.

Scattering from Networks under Strain. The network sample was studied at four different strains: $\lambda_{||} = 1.25, 1.45, 1.60, 1.75$.

Figure 5 displays experimental results for the directions $q_{||}$ and $q_{\perp}$ to the uniaxial strain for the four strains applied. The data were obtained from the transversal Zimm extrapolation as explained above. Fixing the undeformed radius of gyration to the value found for the isotropic sample and keeping the exponent $\nu = {}^1/_2$ (eq 2) the data were fitted with the RPA corrected structure factor (eq 4). The only parameters thereby were the tube diameter d_0 and the content of scissioned chains w_s. The achieved fits are included in Figure 5.

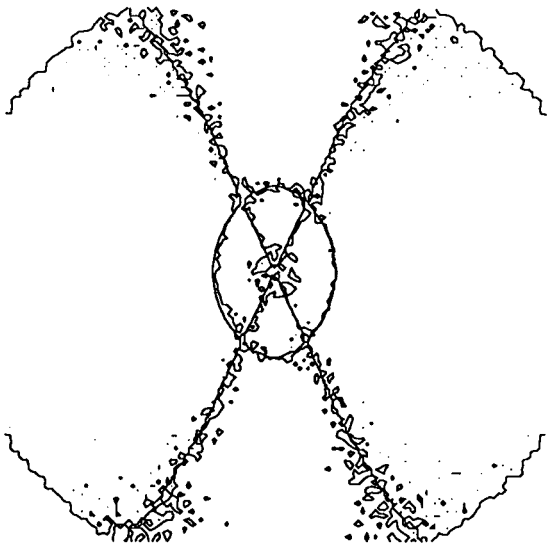

Figure 7. Contour plot of the vanishing difference $\Delta S = S(\vec{q},\lambda = 1.75) - S(\vec{q},\lambda = 1) = 0$, giving the isotropy angle $\phi^* = (65.5 \pm 0.5)°$. Using the definition of the microscopic strain component $\lambda_{||}$ in eq 28, one obtaines $\lambda_{||} = 1.75 \pm 0.05$.

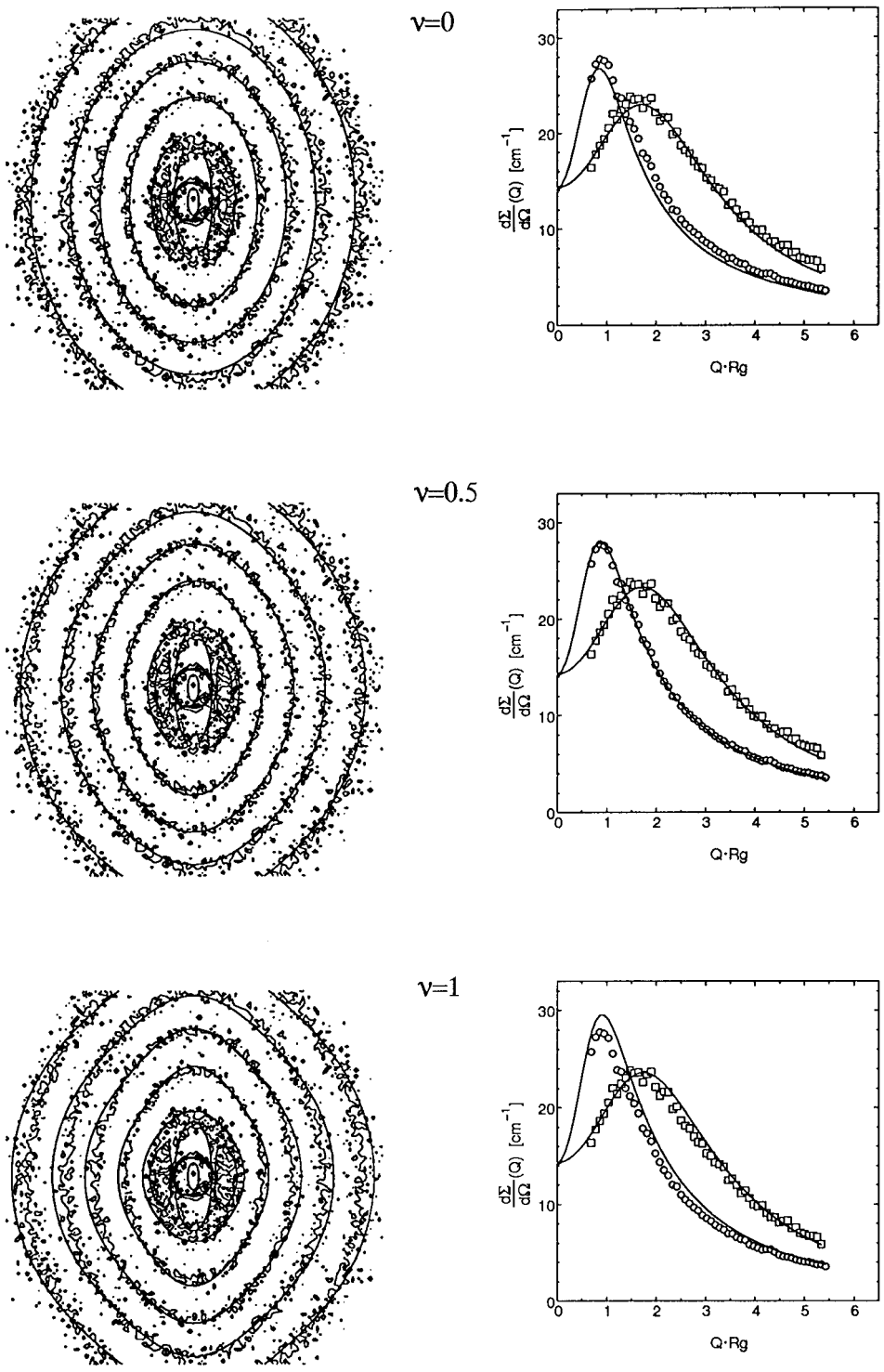

Figure 8. Test of the prediction $\nu = 1/2$. The tube diameter was fixed at 41.5 Å. Both values $\nu = 0$ and $\nu = 1$ are not able to describe the position or the width of the peak. Only the value $\nu = 1/2$ is able to represent the q dependence of the strained data properly.

The theoretical curves describe the scattering data very well, especially peak positions, heights, and forms are in almost complete agreement with experiments. Table 2 summarizes the results. The chain splitting parameter varies insignificantly and corresponds within statistical error to the content derived from the isotropic fit. The data yield a tube diameter, $d_0 = 42 \pm 1$ Å which is equal for all extension ratios.

Figure 6 presents contour plots of the two-dimensional data fits. The obtained parameters are also collected in Table 2 and agree reasonable well with the data from the axes fits. The chain splitting amount was fixed at the averaged value derived by the axes fits. Therewith the parameters obtained from fits of all experimental data in the whole scattering plane confirm the values of the axes fits. Consequently, these parameters are reliable, and the axes fits really represent the agreement between experiments and model. The tube diameter is $d_0 = 41.5 \pm 0.5$ Å in excellent correspondence with the axes fits. The excellent agreement of the theoretical contours with the experimental data is clearly visible. At the largest strain even the onset of typical lozengic patterns is just visible as it was the case in longer homopolymers at larger strains.

Figure 7 shows the contour plot of the difference $\Delta S = S(\vec{q},\lambda) - S(\vec{q},\lambda = 1)$ which gives the microscopic strain component $\lambda_{||}$ directly from measuring the angle ϕ^* between the stretching axis and the line $\Delta S = 0$. Using the definition of λ_ϕ in eq 3, one obtains

$$\lambda_{||} = -{}^1/_2 + \sqrt{\frac{1}{4} + \tan^2 \phi^*} \qquad (28)$$

With $\phi^* = (65.5 \pm 0.5)°$, $\lambda_{||} = 1.75 \pm 0.05$ is identical with the macroscopic strain $\lambda = 1.75 \pm 0.08$ and gives the microscopic proof that the deformation is affine on the length scale of the labeled block. The ease of such a graphical solution was stressed in our previous work.[4]

The values for the tube diameter obtained in this work agree well with the previously published value of $d_0 = 44 \pm 2$ Å of a network consisting of long labeled homopolymers of polyisoprene.

Summarizing the accumulated results, we may conclude that the estimations of the tube diameters in rubberlike networks are consistent. The use of block copolymer systems allows an advantageous investigation of networks of somewhat shorter chains than in ref 4, since any influences of dangling ends can be excluded. The influence of dangling ends which are isotropic or at least less anisotropic than the chains between cross-links due to relaxation processes can be simply reduced by use of long primary chains. This would lead to inconvenient large chains for homopolymer systems and gives rise to a small-angle scattering signal outside the accessible q range.

Additionally, the particular peak structure of the scattering permits a detailed test of the prediction $\nu = {}^1/_2$. Figure 8 shows the results for the three values $\nu = 0, {}^1/_2, 1$. Especially parallel to the stretching direction, neither the value $\nu = 0$ nor the value $\nu = 1$ is able to describe the data properly. The theoretical curves shift the peak position and height, and also the peak width is not reasonably described. The curves were computed using the now well-established tube diameter of $d_0 = 42 \pm 1$ Å for polyisoprene found in long homopolymers at lower cross-link densities[29] and also in this work. Consequently, the influence of cross-links and cross-link fluctuations on d_0 must be small in the range of typical rubberelastic networks, and this value will be used for further discussions. Fits of d_0 using the same fitting procedures but for the deformation exponent the values $\nu = 0$ and $\nu = 1$ yield best-fit tube dimensions $d_0 = 30$ and 50 Å, respectively, and give less agreement with experimental data similar to the curves in Figure 8; only the perpendicular direction is described properly. Statistically, these values for d_0 lie outside of the range of experimental uncertainty, giving rise to an exclusion of both seemingly more natural deformation dependencies of the tube dimensions.

Conclusion

The aim of the presented work was to study topological constraints and microscopic deformations in polymer networks made from HDH polyisoprene copolymers. The actions of cross-links and entanglements were modeled by means of a harmonic deformation dependent constraining potential. This tube model was combined with the RPA method to describe the measured SANS patterns, i.e., the deformation of the correlation peak.

Fits on isotropic data supported the necessity of taking into account a chain splitting during the cross-linking process. The amount of chain scissions clusters around 8%.

The description of the experimental results by the used model confirms the assumptions concerning the introduction of the RPA correction into the Warner−Edwards approach. The use of triblock copolymers permitted an independent and reliable determination of tube dimensions and their deformation in networks made from shorter primary chains and at considerably lower strains than in previous work. The value of the undeformed tube diameter is in good correspondence to those determined earlier.[3,4]

The deformation dependence of the tube diameter was reinvestigated by means of the very sensitive peak structure typical for a copolymer. Both the affine deformation and the strain-independent case $\nu = 0$ can clearly be excluded, whereas $\nu = {}^1/_2$ is confirmed.

Further experiments will be undertaken using the labeled middle block as a molecular probe by varying its length also below the range of the entanglement spacing. By this it should be possible to perform more stringent tests of the predictions of the used model. Especially the case in which the size of the middle block becomes of the order or smaller than the tube dimension is of special interest, and information about the mechanisms of the Rouse reptation transition can be expected.

Finally, we have shown that the developed approach using block copolymers has a promising potential for the investigation of chain conformations and especially confinement effects in complex polymer systems.

Acknowledgment. The authors thank the Institute Leon Brillouin, Saclay, France, and the National Institute of Standards and Technology (NIST), Gaithersburg, MD, for the use of the beamtime. M. Hintzen is gratefully acknowledged for the sample preparation and characterization and F. Boue (Saclay) and C. Glinka (NIST) for stimulating discussions and their help during the SANS experiments. Part of the work was carried out with the support of the EC-HCM Program, Contract ERB CHGECT 920001.

References and Notes

(1) Ullman, R. *Macromolecules* **1982**, *15*, 1395.
(2) Kloczkowski, A.; Mark, J. E.; Erman, B. *Comput. Polym. Sci.* **1992**, *2*, 8.
(3) Straube, E.; Urban, V.; Pyckhout-Hintzen, W.; Richter, D. *Macromolecules* **1994**, *27*, 7681.
(4) Straube, E.; Urban, V.; Pyckhout-Hintzen, W.; Richter, D.; Glinka, C. J. *Phys. Rev. Lett.* **1995**, *74*, 4464.
(5) Doi, M.; Edwards, S. F. *The Theory of Polymer Dynamics*; Clarendon: Oxford, 1986.
(6) Heinrich, G.; Straube, E.; Helmis, G. *Adv. Polym. Sci.* **1988**, *85*, 33−87.
(7) de Gennes, P. G. *Scaling Concepts in Polymer Physics*; Cornell University Press: Ithaca, NY, 1979.
(8) Leibler, L. *Macromolecules* **1980**, *13*, 1602.
(9) Leibler, L.; Benoit, H. *Polymer* **1981**, *22*, 195.
(10) Boue, F.; Daoud, M.; Nierlich, N.; Williams, C.; Cotton, J. P.; Farnoux, B.; Jannink, G.; Benoit, H.; Dupplessix, R.; Picot, C. *Neutron Inelastic Scattering Proceedings*; International Atomic Energy Agency, Vienna, 1977; Vol. 1.
(11) Warner, M.; Edwards, S. F. *J. Phys. A* **1978**, *11*, 1649.
(12) Kim, J. K.; Kimishima, K.; Hashimoto, T. *Macromolecules* **1993**, *26*, 125−136.
(13) Xu, H.; Kitano, T.; Kim, C. Y.; Amis, E. J.; Chang, T.; Landry, M. R.; Wesson, J. A.; Han, C. C.; Lodge, T. P.; Glinka, C. J. *Advances in Elastomers and Rubber Elasticity*; Plenum Press: New York, 1986.
(14) Heinrich, G.; Straube, E. *Acta Polym.* **1983**, *34*, 589−594.
(15) Heinrich, G.; Straube, E. *Polym. Bull.* **1987**, *17*, 255−261.
(16) Richter, D.; Farago, B.; Fetters, L. J.; Huang, J. S.; Ewen, B.; Lartigue, C. *Phys. Rev. Lett.* **1990**, *64*, 1389.

(17) Richter, D.; Butera, R.; Fetters, L. J.; Huang, J. S.; Farago, B.; Ewen, B. *Macromolecules* **1992**, *25*, 6156.
(18) Boue, F.; Bastide, J.; Buzier, M.; Lapp, A.; Herz, J.; Vilgis, T. A. *Colloid Polym. Sci.* **1991**, *269*, 195−216.
(19) Mildner, D. F. R. *Macromolecules* **1983**, *16*, 1760.
(20) Gronski, W.; Hoffmann, W.; Simon, G.; Wutzler, A.; Straube, E. *Rubber Chem. Technol.* **1992**, *65*, 63.
(21) Queslel, J. P.; Thirion, P.; Monnerie, L. *Polymer* **1986**, *27*, 1869.
(22) Maconnachie, A.; Richards, R. *Polymer* **1978**, *19*, 739.
(23) Hadjichristidis, N.; Xu, Z.; Fetters, L. J.; Roovers, J. *J. Polym. Sci., Polym. Phys. Ed.* **1982**, *20*, 743.
(24) Wignall, G. D.; Christer, D. K.; Ramakrishnan, V. *J. Appl. Cryst.* **1988**, *21*, 438.
(25) Capla, M.; Borsig, E. *Eur. Polym. J.* **1980**, *16*, 611.
(26) Charlesby, A.; Pinner, S. *Proc. R. Soc. London A* **1959**, *249*, 367.
(27) Klüppel, M. *J. Appl. Polym. Sci.* **1993**, *48*, 1137.
(28) Westermann, S.; Pyckhout-Hintzen, W.; Richter, D.; Straube, E., in preparation.
(29) Urban, V.; Westermann, S.; Pyckhout-Hintzen, W.; Richter, D.; Straube, E., manuscript in preparation.

MA9602381